

**CHAPTER III**  
**MICROSTRUCTURE EFFECT OF NANOCRYSTALLINE TITANIUM**  
**DIOXIDE PREPARED BY MICROEMULSION TECHNIQUE ON**  
**PHOTOCATALYTIC DECOMPOSITION OF PHENOL**

**3.1 Abstract**

Titanium dioxide ( $\text{TiO}_2$ ) was synthesized in the water-in-oil (w/o) microemulsion system of *n*-heptane/water/sodium bis (2-ethylhexyl) sulfosuccinate (AOT) surfactant. This study reports the effect of microstructure of the synthesized  $\text{TiO}_2$  nanoparticles on the photocatalysis degradation of phenol in an aqueous solution, as compared to commercial  $\text{TiO}_2$  (P25) and  $\text{TiO}_2$  synthesized by bulk precipitation. The results indicated that the rate of phenol decomposition catalyzed by the synthesized  $\text{TiO}_2$  from microemulsion techniques is faster than those of  $\text{TiO}_2$  synthesized by bulk precipitation and commercial P25. This is due to the small crystal size of  $\text{TiO}_2$  prepared by the microemulsion technique. The exposed titanium sites on the surface controlled by the morphology of synthesized  $\text{TiO}_2$  are critical for photocatalytic activity.

**3.2 Introduction**

The excellent chemical and electronic properties of ceramics, semiconductors and metallic catalysts have attracted a great deal of attention in the development of new technologies for the future, *e. g.*, the high activity of metallic catalysts [1-3]. Nano-sized particles possess better physical and chemical properties when compared to bulk materials, in particular for applications using changes in surface properties, due to their larger surface/bulk ratio [3]. Thus, particle size is a crucial parameter for controlling the electronic and chemical properties of materials. Producing so-called "nanoparticles," whose diameter is in the range of 1-30 nm, has become a major interdisciplinary area of research over the past 10 years.

Among metal oxides,  $\text{TiO}_2$  is extremely interesting since it is inexpensive and has been utilized in many industrial applications due to its various unique properties [4-8].  $\text{TiO}_2$  has excellent photocatalytic activity, which can be used to eliminate toxic molecules such as volatile organic compounds (VOCs) in wastewater treatment [6-8]. A conventional method that has been applied to prepare this metal oxide is the precipitation technique [9-11]. Although the precipitation technique is easy, the morphology and size of the metal oxide are difficult to control, resulting in unreliable properties in real applications.

There are many methods that can be used to control the size of nanoparticles. Microemulsion is one of the most interesting techniques that can be successfully used to control the size of various organic and inorganic materials because of their thermodynamic stability in the microenvironment [11-16]. In a previous work [17], the effect of microemulsion on controlling size, phase and structure of synthesized  $\text{TiO}_2$  in reverse micelles of *n*-heptane/water/NaCl/ sodium bis (2-ethylhexyl) sulfosuccinate (AOT) was investigated. The results indicated that increasing salt concentration could effectively control the size of nanometric  $\text{TiO}_2$ , which would lead to uniform dispersion and high crystallinity. Moreover, a large fraction of anatase phase was obtained. Although the synthesized  $\text{TiO}_2$  showed promising properties to enhance the photocatalytic activity of  $\text{TiO}_2$ , further investigation is needed to explain this phenomena. Therefore, this work is focused on the correlation between the morphology of oxide particles, the method of preparation, and the properties of the synthesized materials.

In this study, the effect of the microstructure of  $\text{TiO}_2$  synthesized by microemulsion (*n*-heptane/water/NaCl/ sodium bis (2-ethylhexyl) sulfosuccinate (AOT)) on the photocatalytic degradation of an organic pollutant (phenol) in aqueous solution was investigated. Phenol was selected as a model pollutant because it is a non-volatile and common contaminant present in industrial wastewaters [6-8]. The effect of crystal size, crystal structure, and surface area enhancing adsorption in aqueous phase of the synthesized  $\text{TiO}_2$  on the phenol degradation was studied.

### 3.3 Experimental

#### 3.3.1 Reagents

High purity (98%) anionic surfactant, sodium bis (2-ethylhexyl) sulfosuccinate (Aerosol OT, AOT), was obtained from Fluka (Switzerland). The analytical reagents (AR), 99% *n*-heptane as an oil phase, 99% sodium chloride (NaCl), and 99.5% acetone, were purchased from Lab-Scan (Thailand). Ammonium hydroxide (NH<sub>4</sub>OH, AR grade) was purchased from J.T.Baker (N.J., U.S.A.). Titanium dioxide (TiO<sub>2</sub>, P25) was obtained from Degussa (Frankfurt, GmbH) and 40% hydrofluoric acid (HF) from Riedelde Haën AG. Perchloric acid (56%, HClO<sub>4</sub>) was purchased from Carlo Erba (Italy). All reagents were used without further purification. Deionized water was used for all the experiments.

Titanium tetrachloride solution (TiCl<sub>4</sub>) in concentrated HCl was prepared by dissolving and heating TiO<sub>2</sub> in concentrated aqueous HF solution until a clear solution was obtained. Then, a few milliliters of HClO<sub>4</sub> was added to remove excess HF from the solution. Finally, titanium tetrachloride in concentrated HCl solution was obtained by adding HCl. The reactions are:



#### 3.3.2 Microemulsion Preparation

Microemulsion was prepared by mixing 90 g of 6% wt/wt AOT in *n*-heptane solution with 10 g of aqueous solution of 0.3 M TiCl<sub>4</sub> and NaCl. After mixing for 2 h, the solution was equilibrated at 30°C. Then, the separation of excess water phase and reverse micelle microemulsion (upper phase) was obtained. The clear upper solution indicated that the obtained microemulsion was stable. The microemulsion was then separated to perform the precipitation. The apparent hydrodynamic diameter (micellar size, D<sub>h</sub>) of the microemulsion was determined

using dynamic light scattering (DLS) (Coherent, CA., U.S.A.) at a constant angle of  $90^\circ$ , pinhole of 100, wavelength of 514.3 nm ( $\text{Ar}^+$ , Lazer light source, 100 mW), and a constant temperature of  $30^\circ\text{C}$ . The water content in the microemulsion phase was determined using a coulometer (Metrohm 737 KF, Switzerland). Fifty microliters of microemulsion solution was titrated with a Hydramal Coulomat solution. The water content reported was an average of three runs.

### 3.3.3 Precipitation

The precipitation was carried out by bubbling into the microemulsion an air flow saturated with ammonia, obtained by bubbling air through a concentrated  $\text{NH}_4\text{OH}$  solution, until the pH was 7.0. The precipitate was separated by a high-speed low-temperature centrifuge (Sorvall super T21, DuPont, U.S.A.) at 10,000 rpm for 20 min, washed once with n-heptane, twice with ethanol and acetone, followed by water to remove the remaining surfactant from the precipitated particles. The precipitated particles were dried at  $80^\circ\text{C}$  for 24 h to remove water, and calcined at  $460^\circ\text{C}$  for 5 h prior to their characterization.  $\text{TiO}_2$  was also prepared using bulk precipitation of 0.3 M of  $\text{TiCl}_4$  aqueous solution for sake of comparison with  $\text{TiO}_2$  synthesized by the microemulsion technique.

### 3.3.4 Characterization

X-ray diffraction (XRD) patterns of all titanium dioxide particles were obtained by using a Phillips PW 1830/00 No. SY 1241 diffractometer equipped with a graphite monochromator and a Cu tube for generating a  $\text{CuK}\alpha$  radiation (wavelength 1.5406 Å). Peak positions were compared with standard files to identify crystalline phases.

The titanium dioxide particles were observed using a transmission electron microscope (TEM, Jeol 2010, Tokyo, Japan). The specific surface area of  $\text{TiO}_2$  was measured using a surface area analyzer (Autosorb I, Quantachrom, U.S.A). The titanium dioxide particles were first outgassed to remove moisture and volatile adsorbents under vacuum at  $300^\circ\text{C}$  for 3 h before starting the analysis to determine the surface area. The software Autosorb ANYGAS Version 2.10 was used to analyze the results. The adsorption data were calculated using the Brunauer-Emmett-Teller (BET) equation.

### 3.3.5 Photocatalytic Experiments

The phenol degradation experiments were carried out in a Pyrex reagent bottle as a reactor. The 0.1 dm<sup>3</sup> reaction mixture inside the reactor was maintained in suspension by magnetic stirring. In all experiments, oxygen was bubbled continuously through the solution. A medium pressure mercury vapor lamp was used as the light source. All the experiments were carried out at 28.0 ± 0.1°C. The concentration of TiO<sub>2</sub> in suspension was 1.0 g·dm<sup>-3</sup>. The initial pH of dispersion was adjusted to 3.0 by the addition of hydrochloric acid. To separate the particles prior to the analysis, the sample solutions were centrifuged at 10,000 rpm for 20 min. Then, the supernatants were filtered 2 times through 0.25 µm pore size cellulose acetate filter. The phenol concentration was determined by HPLC (Hewlett Packard series) equipped with a UV-VIS detector at 270 nm, for the detection of phenol, and ODS spherisorb column (150 mm in length, i.d. 4.6 mm and 5 µm particle diameter). The mobile phase was a mixture of 1:1 volume ratio of water to acetonitrile with a flow rate of 1.0 mL/min.

## 3.4 Results and Discussion

### 3.4.1 Effects of Salt on Micellar Size and Water Content

The effect of salt on water content and size of reverse micelles was investigated by varying the concentration of NaCl from 0 to 6 wt%. When the concentration of NaCl increased, the water content and micellar size decreased, as shown in Fig. 3.1 and Fig. 3.2, respectively. The micellar size decreased from 32 nm to 8 nm with the addition of 6 wt% NaCl. Increasing NaCl concentration increased the association of counter ions with the surfactant head groups. As a result, the repulsive interaction between the head groups decreased resulting in a decrease in micellar size.

### 3.4.2 Synthesis of Titanium Dioxide Particles In Microemulsions and Their Characterization

The prepared titanium dioxide was calcined at 460°C for 5 h and was subsequently characterized by a BET specific surface area analyzer, TEM and XRD. Fig. 3.3 shows the XRD results of TiO<sub>2</sub> obtained from bulk precipitation (a), microemulsion (b-d), and commercial P25 (e). The XRD data indicated that TiO<sub>2</sub> was present in the anatase structure for the samples prepared with microemulsion in the presence of salt as well as in TiO<sub>2</sub> from the bulk precipitation, while 21% and 18% of rutile phase was observed together with anatase for the commercial P25 and the sample synthesized from microemulsion in the absence of salt, respectively. The XRD experimental peaks of TiO<sub>2</sub> synthesized from microemulsion were characteristically broad, which is expected for nanoparticles.

Figure 3.4 shows the TEM results for the various titanium dioxide samples. The P25 titanium dioxide (Fig. 4a) had an average diameter of 30 nm, while the TiO<sub>2</sub> powders synthesized using microemulsion with various salt concentrations (Fig. 4b-4d) had a smaller diameter and were uniform. The larger the salt addition, the smaller the crystal size. The average crystal size decreased from 20 nm to 7 nm as NaCl concentration was increased from 0 to 6 wt%. The largest crystal size with high dispersion in the grain size was obtained from the bulk precipitation. Table 3.1 summarizes the data obtained from DLS, TEM and BET specific surface area measurements. The TEM results indicated that the size of synthesized TiO<sub>2</sub> was controlled by the size of the micelles, as measured by DLS, and the corresponding water content. As expected, the smaller the size of the TiO<sub>2</sub> particles, the larger the associated BET surface area.

### 3.4.3 Photocatalytic Degradation of Phenol

#### *3.4.3.1 The effect of initial concentration of phenol on the kinetics of the photocatalytic process*

Fig. 3.5 shows the degradation time of different initial concentrations of phenol ranging from 50-150 ppm with TiO<sub>2</sub> synthesized from the microemulsion technique (4 wt% NaCl at pH = 3.0). The initial rates of photocatalytic degradation were obtained based on the Langmuir-Hinshelwood kinetics;

$$\frac{1}{r_0} = \frac{1}{k} + \left( \frac{1}{kK} \right) \frac{1}{c_0} \quad (3.3)$$

The plot of  $1/r_0$  and  $1/C_0$ , where  $r_0$  and  $C_0$  are the initial rate of photodegradation and initial concentration of phenol, were investigated (Fig. 3.6). From the plot, the rate constant ( $k$ ) and equilibrium adsorption constant ( $K$ ) were estimated, which are  $2.16 \text{ mg}\cdot\text{dm}^{-3}\cdot\text{min}^{-1}$  and  $24.90 \text{ dm}^{-3}\cdot\text{min}$ , respectively.

The results agreed well with the kinetics and reaction mechanism of phenols on irradiated  $\text{TiO}_2$ , studied by O'Shea *et al.* [18], where the extent of the photodegradation depends on their reactivity towards the photogenerated  $\text{OH}^*$  radicals and hydrogen substitution [8].

#### 3.4.3.2 The effect of microstructure of $\text{TiO}_2$ on the photocatalytic degradation of phenol

Figure 3.7 shows the effect of the different features (size, surface area, and phase) of  $\text{TiO}_2$  samples on the photocatalytic degradation of phenol. The photodegradation test was carried out at the initial phenol concentration of 50 ppm with a load of  $0.1 \text{ g}\cdot\text{dm}^{-3}$  of  $\text{TiO}_2$ . The results yielded the highest catalytic rate of phenol decomposition with the smallest crystal size of  $\text{TiO}_2$ . The smaller size of the particles provided a larger surface-to-volume area, which can increase the number of the active sites for the reactant molecules.

In addition, a change in the mean crystal size also revealed the fraction of exposed titanium sites to reactant molecules and the chance for electrons and holes to reach the surface and react with phenol. Accordingly, the highest rate of photodegradation was obtained from the  $\text{TiO}_2$  particles with smallest size. The degradation rate of phenol on  $\text{TiO}_2$  synthesized from microemulsion with 6 wt% NaCl was compared with the commercial P25 and  $\text{TiO}_2$  prepared from the bulk precipitation (Fig. 3.8). The  $\text{TiO}_2$  synthesized from microemulsion showed the fastest rate of phenol decomposition. This might be attributed to the difference in uniformity and nanocrystalline structure of the particles. No significant differences in the degradation rate were observed between the bulk precipitate and P25, although

P25 has a smaller crystal size than TiO<sub>2</sub> from bulk precipitation. This can be attributed to the different TiO<sub>2</sub> phases present in the samples; in fact, the TiO<sub>2</sub> prepared from bulk precipitation was pure anatase, which is catalytically highly active under the irradiation of UV-light, while the rutile phase found in P25 is not catalytically active [19]. To clarify the microstructural effect of TiO<sub>2</sub> particles on enhancing the phenol decomposition rate, the dependence of the apparent turnover frequency (TOF) number on BET surface area and mean crystal size was studied and the results are reported in Figs 3.9 and 3.10. TOF was defined as the amount of phenol converted per unit time and per TiO<sub>2</sub> loading. The TOF profile clearly shows the relation of the exposed fraction of TiO<sub>2</sub> sites to the activity. As the crystal size of anatase increased, the TOF number decreased. TOF was maximum for the smallest crystal size. This trend is in agreement with the increase of TiO<sub>2</sub> active sites with increasing the surface-to-bulk ratio.

### 3.5 Conclusions

The formation of nanometer-sized titanium dioxide particles in the microemulsion system of *n*-heptane/TiCl<sub>4</sub>/NaCl/AOT anionic surfactant reacted with NH<sub>3</sub> was studied. NaCl concentration was varied to control the size of TiO<sub>2</sub>. The size of micellar reactors and the amount of NaCl in the microemulsion control the growth of the TiO<sub>2</sub> by thermodynamic stabilization, where the reverse micelle acts as a constraint. This also controls the growth and structure of the titanium dioxide. Titanium dioxide synthesized in microemulsion, P25, and bulk precipitate were different in their characteristics and particle size. The preparation technique affected the TiO<sub>2</sub> microstructure. Titanium dioxide obtained from bulk precipitation had a broad distribution of particle size, with a larger average particle size. P25 had a smaller size (30 nm) but contains also TiO<sub>2</sub> in rutile form and not only anatase. Titanium dioxide synthesized in microemulsion was pure, crystalline anatase phase and possessed the smallest particle size (7-20 nm) and the highest specific surface area, showing therefore the best photocatalytic activity in phenol degradation. In fact, TiO<sub>2</sub> synthesized from microemulsion showed the fastest rate of phenol



decomposition related to its smaller crystal size and higher surface area to unit volume. The change in the mean crystal size clearly determined the fraction of the exposed titanium active sites to reactant molecules and increased the chance for electrons and holes to reach the surface and react with phenol.

### 3.6 Nomenclature

$\theta$  theta, degree

$k$  rate constant,  $\text{mg}\cdot\text{dm}^{-3}\cdot\text{min}^{-1}$

$K$  equilibrium adsorption constant,  $\text{dm}^{-3}\cdot\text{min}$

$C$  phenol concentration

$D$  Micellar size

*Subscript*

$o$  initial condition

$h$  hydrodynamic system

### 3.7 Acknowledgements

This work was financially supported by the Golden Royal Jubilee Program, the Thailand Research Fund and the University of Rome "Tor Vergata." The authors would like to express sincere thanks for National Metal and Materials Technology Center, Thailand, for characterization using TEM. Finally, I would like to give special thanks for Dr. Angkhana Jaroenworoluck, Dr. Maria Luisa Grilli, and Dr. Elisabetta Di Bartolomeo.

### 3.8 References

1. E. Traversa: Intelligent ceramic material for chemical sensors, *J. Intelligent Material System and Structure* 6, 860-869 (1995).

2. N. Barsan and U. Weimar: Conduction model of metal oxide gas sensors, *J. Electroceramics* 7, 143-167 (2001).
3. T. Trindade, P. O. Brien, and N. L. Pickett: Nanocrystalline semiconductors: synthesis, properties and perspectives, *Chem. Materials* 13, 3843-3858 (2001).
4. L. Shi, C. Li, H. Gu, and D. Fang: Morphology and properties of ultrafine SnO<sub>2</sub>-TiO<sub>2</sub> coupled particles, *Materials Chemistry and Physics* 62, 62-67 (2000).
5. K. Zakrzewska: Mixed oxide as gas sensors, *Thin Solid Films* 391, 229-238 (2001).
6. I. Ilisz and A. Dombi: Investigation of photodecomposition of phenol in near-UV-irradiated aqueous TiO<sub>2</sub> suspensions. II. Effect of charge-trapping species on product distribution, *Applied Catalysis A: General* 180, 35-45 (1999).
7. L. J. Alemany, M. A. Banares, E. Pardo, F. Martin, M. G. Fereres, and J. M. Blasco: Photodegradation of phenol in water using silica-supported titania catalyst, *Applied Catalysis B: Environmental* 13, 289-297 (1997).
8. A. M. Peiro, J. A. Ayllon, J. Peral, and X. Domenech: TiO<sub>2</sub>-photocatalyzed degradation of phenol and ortho-sustituted phenolic compounds, *Applied Catalysis B: Environmental* 30, 359-373 (2001).
9. K. C. Song and Y. Kang: Preparation of high surface area tin oxide powders by a homogeneous precipitation method, *Materials Letters* 45, 283-289 (2000).
10. E. Dalas, S. Sakkopoulos, E. Vitoratos, and L. Kobotiatis: Synthesis of palladium nanoparticles in water-in-oil microemulsions, *J. Materials Science* 20, 5456-5460 (1993).
11. S. Han, H. Yang and J. Kim: Preparation and properties of vanadium-doped SnO<sub>2</sub> nanocrystallites, *Sensors and Actuators B* 66, 112-115 (2000).
12. M. Wu, D. Chen and T. Huang: Synthesis of Au/Pd bimetallic nanoparticles in reverse micelles, *Langmuir* 17, 3877-3883 (2001).
13. K. C. Song and J. H. Kim: Preparation of nanosized tin oxide particles from water-in-oil microemulsions, *J. Colloid Interface Science* 212, 193-196 (1999).
14. F. Deduigne, L. Jeuniau, M. Wiame, and J. B. Nagy: Synthesis of organic nanoparticles in different w/o microemulsion, *Langmuir* 16, 7605-7611 (2000).
15. H. H. Ingelsten, R. Bagwe, A. Palmqvist, M. Skoglundh, C. Svanberg, K. Holmberg, and D. O. Shah: Kinetics of the formation of nano-sized platinum

- particles in water-in-oil microemulsions, *J. Colloid Interface Science* 241, 104-111 (2001).
16. F. T. Quinlan: Reverse micelles synthesis and characterization of ZnSe nanoparticles, *Langmuir* 16, 4049-4051 (2000).
  17. C. Saiwan, S. Krathong, T. Anukunprasert, and E. A. O'Rear (III): Nanotitanium dioxide synthesis in AOT microemulsion system with salinity scan, *J. Chem. Eng. Japan* 37, 279-285 (2002).
  18. K. E. O'Shea and C. Cardona, Hammett study on the TiO<sub>2</sub>-catalyzed photooxidation of para-substituted phenols: a kinetic and mechanistic analysis, *J. Organics Chemistry* 59, 5005-5009 (1994).
  19. E. J. Kim and H. Hahn, Microstructure and photocatalytic activity of titania nanoparticles prepared in nonionic w/o microemulsion, *Materials Science Engineering A* 303, 24-29 (2001).

**Table 3.1** Comparison of properties obtained from different techniques

	<i>Crystal size</i>	<i>Surface area</i>
	<i>By TEM, nm</i>	<i>by BET, m<sup>2</sup>.g<sup>-1</sup></i>
Bulk Precipitation	57	6
P25	30	41
0% NaCl	20	60
4% NaCl	8	63
6% NaCl	7	123

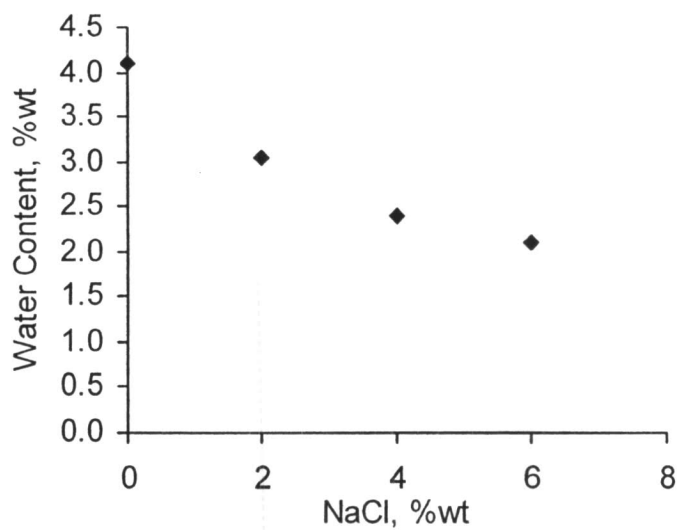


**Figure 3.1** Effect of NaCl on water content in reverse micelle microemulsion.

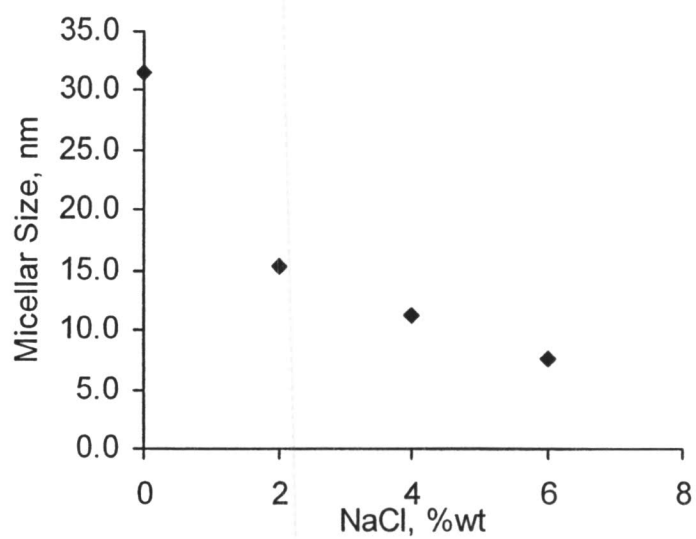


**Figure 3.2** Effect of NaCl on micellar size of reverse micelle microemulsion.

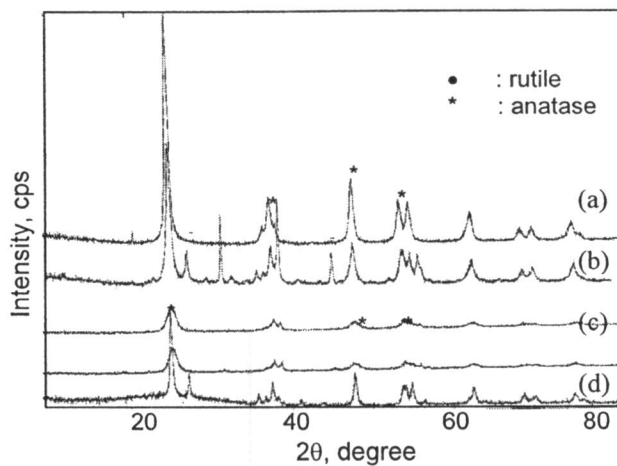


**Figure 3.3** XRD patterns of  $\text{TiO}_2$  from different preparation techniques: (a) bulk precipitation; (b) microemulsion in the absence of NaCl; (c) microemulsion with 4 wt% NaCl; (d) microemulsion with 6 wt% NaCl; and (e) commercial P25.

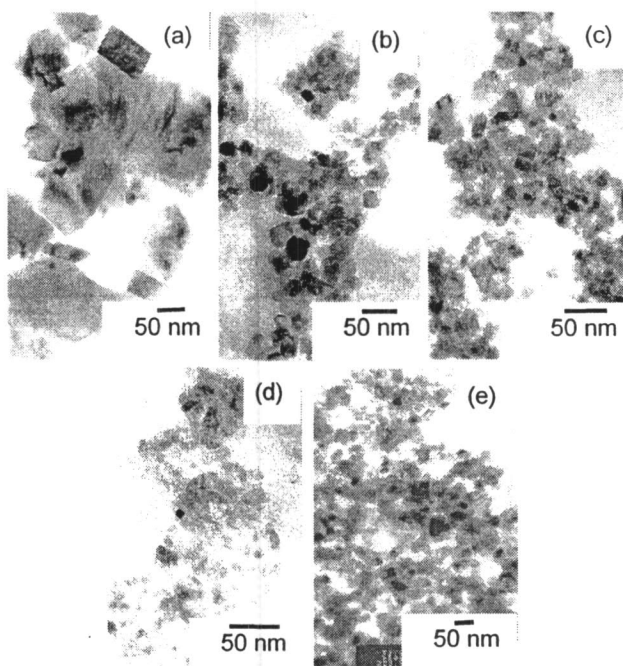


**Figure 3.4** TEM results of  $\text{TiO}_2$  from different techniques: (a) bulk precipitation; (b) microemulsion in the absence of NaCl; (c) microemulsion with 4 wt% NaCl; (d) microemulsion with 6 wt% NaCl; and (e) commercial P25.

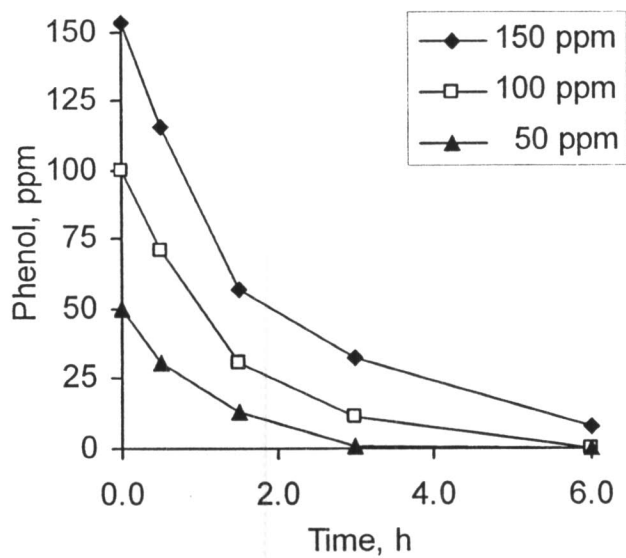


**Figure 3.5** Photocatalytic degradation rate of phenol on  $\text{TiO}_2$  synthesized from microemulsion with various initial concentrations of phenol.

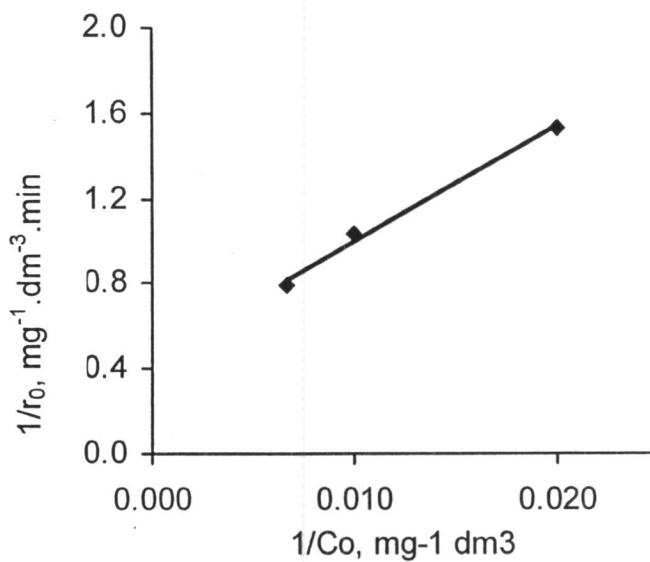


**Figure 3.6** Plot of the inverse initial rate of photocatalytic degradation with respect to the inverse of initial concentration of phenol.

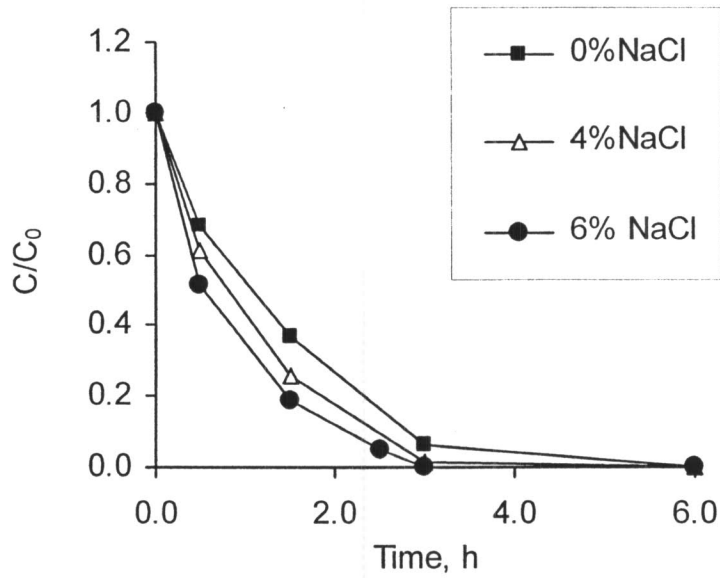


**Figure 3.7** Photocatalytic degradation rate of phenol:  $\text{TiO}_2$  synthesized from microemulsion with various NaCl concentrations. Phenol concentration was 50 ppm and  $\text{TiO}_2$  was  $0.1 \text{ g}\cdot\text{m}^{-3}$ .

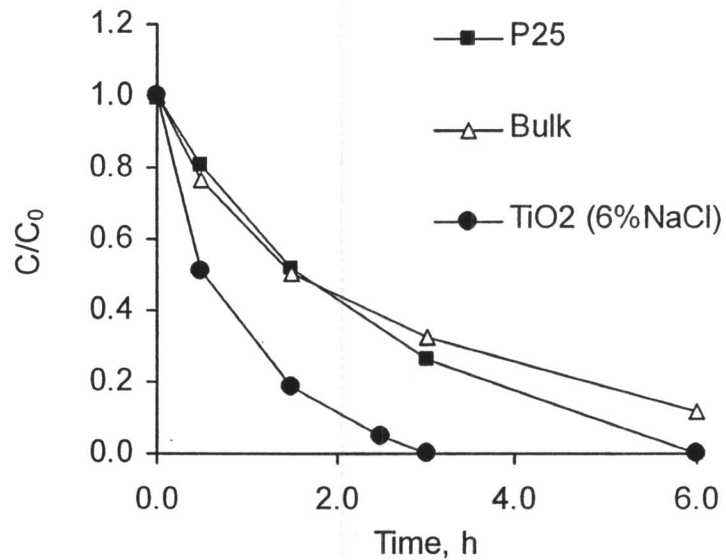


**Figure 3.8** Photocatalytic degradation rate of phenol:  $\text{TiO}_2$  synthesized from microemulsion (6 wt% NaCl) compared with P25 and the bulk precipitation.



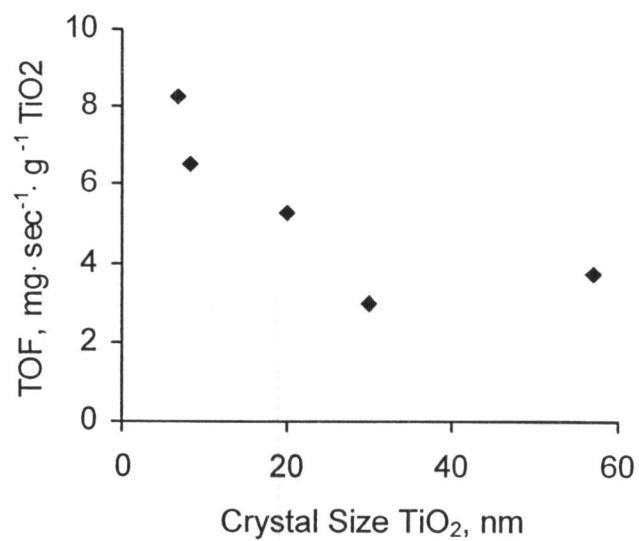


Figure 3.9 TOF as a function of mean crystal size of TiO<sub>2</sub>.

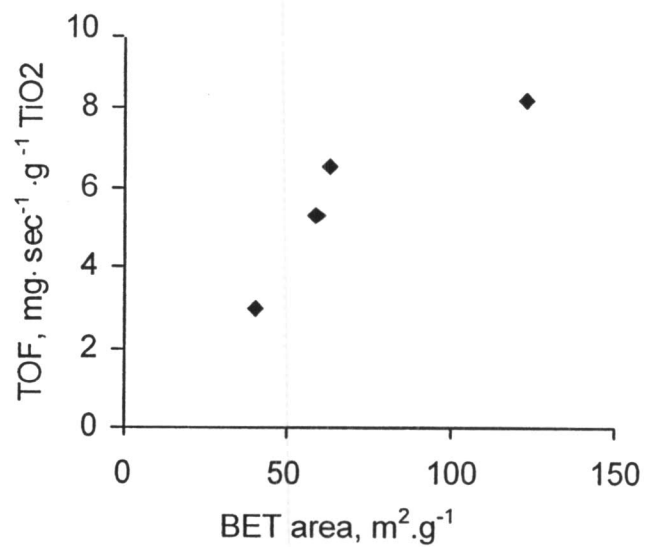


Figure 3.10 TOF as a function of BET surface area of TiO<sub>2</sub>.